https://doi.org/10.48048/tis.2022.5615

Simulation and Comparative Study of Resonant Tunneling Diode

Yashvi Shah[*], Isha Kapoor, Purva Singhvi, Babita Birua and Rutu Parekh

VLSI and Embedded Systems Group, Dhirubhai Ambani Institute of Information and Communication Technology, Gandhinagar 382007, India

([*]Corresponding author's e-mail: yashvi4100@gmail.com)

Received: 6 May 2021, Revised: 30 June 2021, Accepted: 7 July 2021

Abstract

This paper studies and investigates the effect of physical and electrical parameters on double, triple and six barrier resonant tunneling diodes (RTD). The materials used for quantum well and barriers are Gallium arsenide (GaAs) and Aluminium gallium arsenide (AlGaAs), respectively. The parameters that were reasoned and studied include conduction band, current density, transmission coefficient and resonance energy. The above parameters were studied by changing bias voltage, temperature, barrier width and doping concentration. From the simulations performed it is observed that for double barrier RTD the peak current density is observed at 0.2 V and the valley current density is observed at 0.3 V, whereas for a triple barrier RTD the peak current density is observed at 0.015 V and the valley current density is observed at 0.06 V. The value of transmission coefficient for double barrier RTD decreases especially after bias applied is more than resonant bias (0.2 V). The effect of increasing bias leads to a decrease in the resonance level in the conduction band. The width of resonance energy decreases with the increase in barrier width. With increase in number of barrier the number of resonance level increases which leads to an increasing peaks in the transmission coefficient curve. The effect of increasing temperature leads to higher current and more resonance energy. With the thickening of barrier width, less transmission of electrons occurs leading to a reduced current density. When the barriers are increased the negative differential region (NDR) is achieved at low voltages.

Keywords: Resonant tunneling diode, Double barrier, Triple barrier, Six barrier

Introduction

As the field of nanotechnology and nanoscience widens, significant progress is observed in the field of quantum devices. The quantum mechanical wave nature of electrons is anticipated to emerge in nanometre-scale semiconductor structures which have resulted in the formulation of various semiconductor devices. Resonant tunneling diode (RTD) is a diode that works on the principle of quantum mechanical tunneling, which exploits electron wave resonance in multi-barrier hetrostructures [1]. In RTD's, electrons can tunnel through some resonant states at certain energy levels. Quantum tunneling through barriers of nanometer-scale thickness is a very speedy process, as a consequence RTD is capable of performing ultra-high-speed operations [2]. RTD exhibits negative differential resistance and various physical properties that make RTD useful in reducing power consumption of analog and digital circuits, simplifying logic circuits, memory applications, high-frequency applications like - oscillators, pulse generators, mixers and terahertz emitter [3-6]. RTD can achieve a maximum frequency of 2.2 THz which finds its application in wideband secure communications, image processing for low visibility environment, high-resolution radar, and fields of defense and security [7]. With the introduction of the light absorption layer, RTD is also useful in optical communications [8]. RTD's application is curbed by its highly sensitive structure and fabrication process which results in poor consistency on the substrate [9].

The detailed study on RTD was carried out by [10]. Sollner *et al.* [11] outlined a negative differential resistance with a comparatively large peak to valley ratio. These gained attention among researchers and have been studied by many researchers theoretically and experimentally over the past several years. The research is primarily done on double barrier RTD whereas only a few works concentrated on multiple-barrier RTD namely triple barrier. Transmission coefficient and resonance conditions were studied in the 1-dimensional double, triple and quintuple barrier structures [12]. A fully self-consistent Non-Equilibrium Green Function (NEGF) calculation of transmission coefficient, I-V

characteristics, and current noise spectral density in double barrier RTD were presented in [13]. Klimeck [14] discusses in-depth various simulations of different parameters of single and double barrier RTD in his tutorials. Singh *et al*. [15] investigated the effect of barrier length and doping concentration on AlGaAs-GaAs RTD. Rong *et al.* [16] theoretically model triple barrier RTD based on AlGaN/GaN heterostructures. Physical simulation of Gallium nitride (GaN) based double barrier quantum well device was done by Zaharim *et al.* [17] which studied the relationship between current-voltage (I-V) characteristics, particularly negative differential region (NDR) concerning variation in barrier composition, well width and barrier thickness. Almansour and Dakhlaoui [18] studied the effect of applied bias on current density. Almansour [19] theoretically studied the electronic properties of double barrier and triple barrier RTD. Optical and electronic transport properties of AlSb/GaInAsSb double barrier RTD had been investigated in [20]. Sawai and Narahara [21] studied the analysis of multiphase oscillation using a closed RTD-oscillator lattice by employing both numerical and experimental methods and examined the usage of an RTD-based cellular neural network in high-speed and highly functional image processors. Also recently Nishida *et al.* [22] used single RTD oscillator to propose a simple coherent detection system which can reduce the size and power consumption of various THz systems.

RTD can be formulated in 3 ways: The Wigner equation, the NEGF scheme and the Schrodinger equation methodology [23]. Quantum transport in nano devices can be formulated using the NEGF approach. NEGF methods are consistently used to calculate current and charge densities in nanoscale (both molecular and semiconductor) conductors under bias [24,25]. The simulation in this paper is supported by the NEGF which furnishes a powerful conceptual and computational framework for treating quantum transport. The use of NEGF incorporates scattering and coherence loss.

In this paper, we have extensively investigated and simulated range of parameters and discussed tradeoffs between physical and electrical parameters of RTD. Output parameters such as conduction band, current density, transmission coefficient and resonance energy are simulated and investigated by changing the bias voltage, temperature, doping and barrier width for double, triple and six barrier RTD's. This will enable the reader and the research community who are engaged on the use of RTD's and its circuit design to have a better understanding of RTD characteristics and scope of applications. The physics behind the tradeoff of parameters like (changing the bias voltage, temperature, doping and barrier width) can be well understood from the simulation results.

RTD design and simulation framework

The RTD consists of various structures such as a single barrier or multi-barrier, but its most basic configuration is that of a double barrier. This double barrier structure consists of a quantum well with discrete energy states between 2 barriers [26]. The most common combination used is Gallium Arsenide - Aluminum Gallium Arsenide (GaAs-AlGaAs). The barriers (AlGaAs) and the well (GaAs) are sandwiched between heavily doped, narrow energy-gap materials as shown in **Figure 1(A)**, which usually are the same as the well layer. Adjoining the barriers, there are thin layers of undoped spacers to ensure that dopants do not diffuse to the barrier layers. Similarly, **Figures 1(B)** and **1(C)** shows the triple barrier and six barrier RTD. It is studied that the electron's wavelength is equivalent to quantum well's proportions (5 - 10 nm). In consequence, the electron's wave nature results in phenomena like quantum tunneling, forming the basis of the working of RTD [15].

To study the tunneling effect, the positive and negative biases are applied to the collector and emitter end, respectively as shown in **Figure 1(A)**. As this bias voltage (applied at the collector end i.e. positive bias) increases, electrons flow from the emitter to the collector. The current increases almost linearly and attains its peak when the emission region conduction band is at the same energy as the resonant level. A further increase in the bias voltage causes a sharp drop in the current because the resonant level falls below the emission region's conduction band and hence negative differential resistance is observed due to a decrease in current.

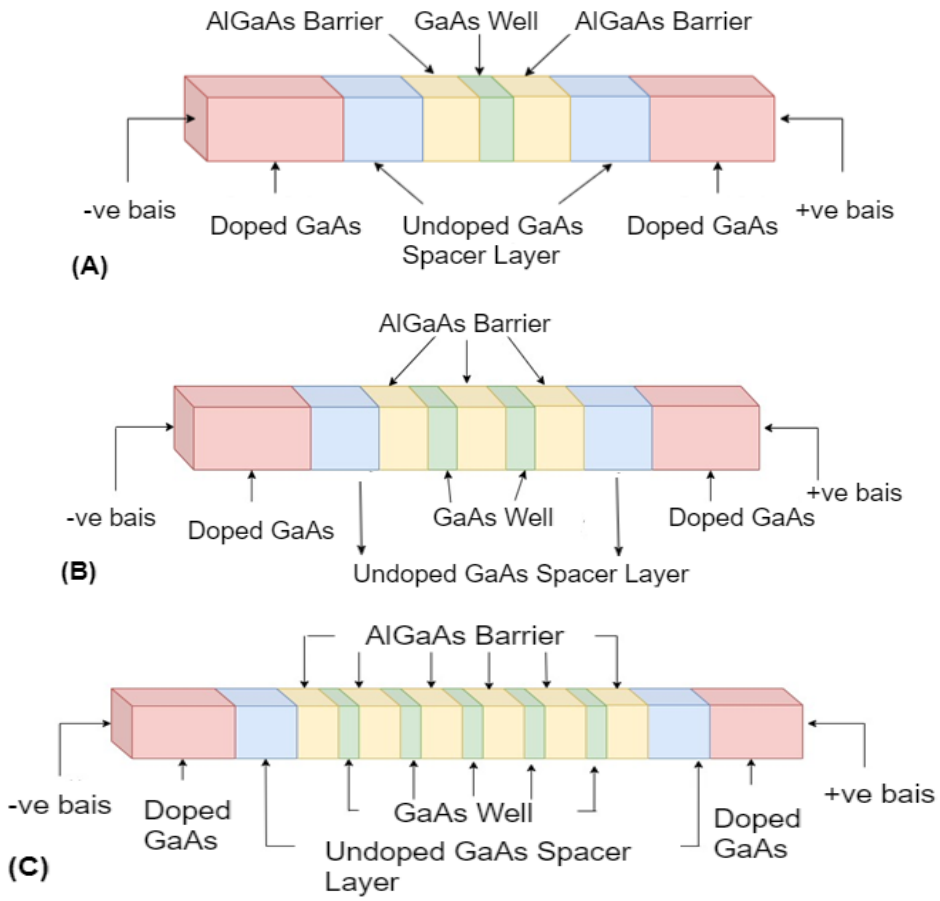

Figure 1 (A) Double barrier RTD, (B) triple barrier RTD and (C) six barrier RTD.

The simulations have been carried out on nanoHub with the help of RTD simulation with NEGF tool. Results have been performed on typical $Al_xGa_{1-x}As/GaAs/Al_xGa_{1-x}$ RTD. The standard parameters are barrier width and well width equals to 5 nm, the width of the contacts (i.e. doped GaAs as shown in **Figure 1**) and spacers (i.e. undoped GaAs spacer layer as shown in **Figure 1**) are kept to be 30 and 10 nm, respectively. The standard temperature is taken to be 300 K and the contacts are doped at $1.0e^{18}$ cm^{-3}. **Table 1** depicts the input parameters used for simulation purpose [27].

Table 1 Input parameter for simulation of RTD.

Input parameters	Values
Device	2-barrier device, 3-barrier device and 6-barrier device
Energy band model	Effective mass model
Potential model	Thomas-Fermi
Quantum charge	Off
Lattice constant	0.2833 nm
Undoped spacer (10 nm)	GaAs
Contact (30 nm)	GaAs
Well (5 nm)	GaAs
Barrier (5 nm)	AlGaAs

Input parameters	Values
Number of voltage points	21
Semi classical charge region (dSC)	10 nm
Equilibrium region (dEQ)	0 nm
Reservoir relaxation model	Exponentially damped
Reservoir relaxation energy	6.6 meV
Decay length	6.6 meV
Poisson criterion	5 meV
Temperature	200, 300 and 400 K
Barrier width	2, 5, 10 and 15 nm
Bias (V)	0.0 - 0.5 V

Results and discussion

The simulation results are shown below for various characteristics such as conduction band, current density, transmission coefficients and resonance energy. The results are simulated at varying bias voltage, temperature, doping concentration and barrier widths.

Double barrier RTD

As shown earlier in **Figure 1(A)**, structure of the double barrier RTD consists of a well sandwiched between 2 barriers that are implanted between the 2 spacers. The spacers are then connected with contacts on either side.

Conduction band

When no voltage is applied, both the emitter and the collector are at the same energy levels. The effect of change in bias voltage on conduction band energy can be seen in **Figure 2(A)**. Here, the bias has been varied from 0 to 0.5 V. On increasing the bias, it can be observed that the conduction band energy and the collector energy level decrease simultaneously. Resonance energy levels decrease when bias is increased as can be observed from **Figure 2(A)**. When the bias is applied, electrons are electrically injected from the emitter into the quantum well. In the collector (near the top contact surface), photo-created holes drift and diffuse, accumulating on the collector/barrier surface and eventually tunneling into the well. Undoubtedly, the transport is through the lowest bound state in the quantum well. The conduction band energy decreases as the applied voltage is increased because the bound level is lowered as the voltage is applied [28]. On further increasing the bias voltage, the conduction band energy level falls below the emitter level. Hence, it can be concluded that conduction band energy is inversely proportional to bias.

With an increase in barrier width, conduction band energy decreases as shown in **Figure 2(B)**. The reason behind this is that when the barrier width is increased, the confinement in the quantum well becomes stronger and increases the electron residence time in the conduction band. Here, the barrier width has been varied from 2 to 15 nm. Moreover, conduction band energy varies in the same way for the well width. Klimeck [14] also studied this behavior of the conduction band energy. Thus, it can be said that with increasing barrier width, conduction band energy decreases.

The effect of the doping concentration of contacts on conduction band energy can be observed in **Figure 2(C)**. Here, doping concentration has been varied from $1.0e^{18}$ up to $30.0e^{18}$ cm^{-3}. Both the contacts have uniform doping concentration. On increasing the doping concentration of contacts, electrons diffuse from high-density contacts to low doping regions. Potential floats up and starts to repel the electrons as a result of high doping concentration. Moreover, as the doping concentration increases, the overall potential rises above the Fermi levels. Also, this change in doping concentration produces the "mountain-like" potential shape. The results obtained by Klimeck [14] are consistent with our observations.

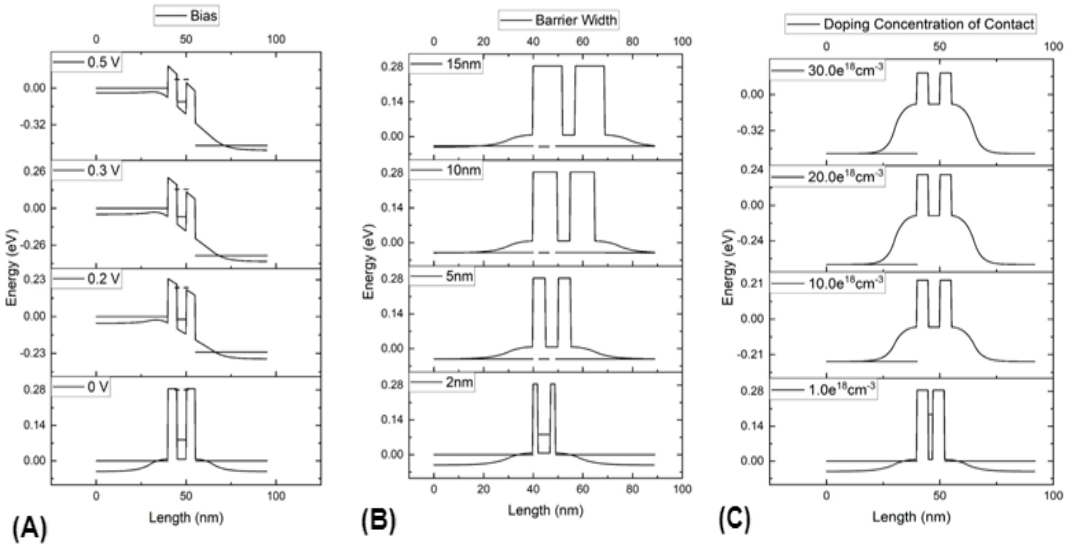

Figure 2 Energy vs length (A) varying bias, (B) varying barrier width and (C) varying doping concentration.

Current density

In **Figure 3(A)**, the current density is depicted as a function of the applied bias voltage. As the bias voltage is increased the resonant energy levels decrease as shown in **Figure 2(A)**. When the minimum of the conduction band of the emitter and the resonant level of the well are aligned the tunneling probability of the electrons increases, leading to a maximum current. After reaching its maximum, the current density decreases sharply and the minimum valley current is obtained which marks the appearance of the negative differential region (NDR). The current decreases because the resonant energy level falls below the conduction band of the emitter and hence no transmission of electrons. These observations are consistent as observed by Almansour and Dakhlaoui [18]. It can be seen from **Figure 3(A)** that there are 3 regions, 2 positive differential regions (PDR 1 and PDR 2) and 1 NDR. PDR 1 region as depicted is from 0 to approximately 0.2 V, whereas the PDR 2 region is above 0.3 V. The NDR region is sandwiched between the 2 PDR regions [2]. The peak current density is approximated to 3,165 A/cm^2 at 0.2 V whereas the peak current density as observed by Almansour is to 4,336 A/cm^2 at 0.225 V [19]. The valley current density is approximated to 1,286 A/cm^2 at 0.3 V whereas the valley current density as observed by Almansour [19] is 1,860 A/cm^2.

Additionally on varying temperature, **Figure 3(B)** shows that the increase in temperature results in an essentially constant peak current, a slightly increasing peak voltage and an increasing valley current [29]. The valley current is observed to increase due to an increase in thermionic emissions at high temperatures. The peak to valley current ratio (PVR) observes a strict degradation because of a high valley current.

Furthermore, **Figure 3(C)** shows the effect of barrier width on the current density at 300 K temperature. A significant decrease in peak current density can be observed due to a decrease in tunneling as the width is increased [30]. The reduction in PVR is obtained because increasing the barrier width would allow the electrons more time to stay in the well, and hence would require a specific amount of energy to tunnel through it, which reduces the tunneling probability resulting in a low current density [15].

Moreover, **Figure 3(D)** depicts the effect of increasing the doping concentration of contact on the current density where the barrier width and the well width are 5 nm. Both the contacts have uniform and same doping levels. The increase in doping concentration at the contacts shifts the Fermi level in the emitter. The minimum peak voltage is obtained with a higher doping concentration which can be seen from **Figure 3(D)** and is consistent with Sanyal and Sarkar [31] observations. The current density starts increasing rapidly when the doping is increased because the amount of charge carriers increases. The maximum current density is observed when the doping concentration is maximum. The graphs and the results obtained are congruent with the results obtained by Singh *et al.* [15].

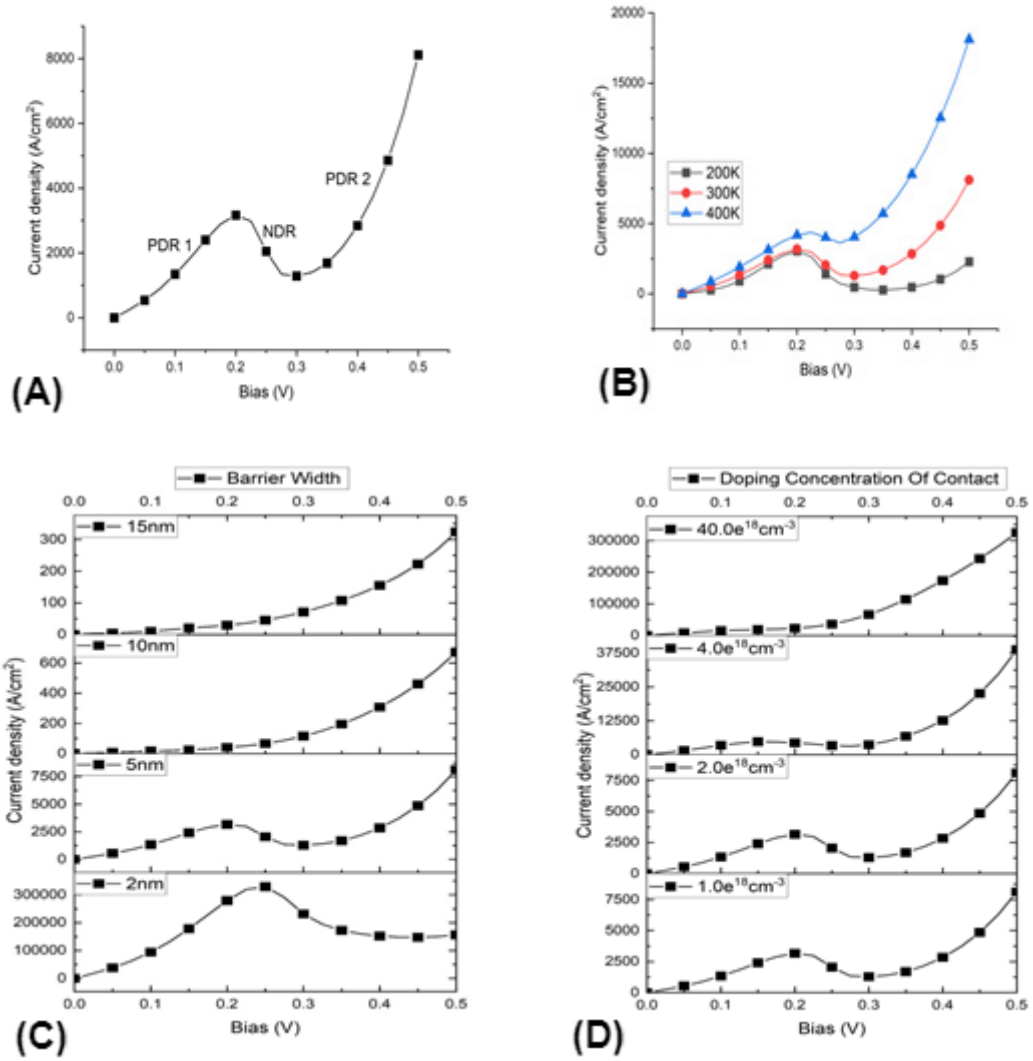

Figure 3 Current density vs bias voltage (A) varying bias, (B) varying temperature, (C) varying barrier width and (D) varying doping concentration.

Transmission coefficient

Transmission coefficient is a probability by which electrons can tunnel through potential barrier. Quantum transmission of double barrier or more can be equal to 1 at some energies, this is due to the presence of resonant states in the well region. **Figure 4** shows energy versus transmission coefficient plots, it can be observed that the transmission spectrum is Lorentzian-like in shape near resonance energies which is also analytically proven [12].

To study the impact of increasing bias on energy versus transmission coefficient, stimulations were done at 4 different biases. From **Figure 4(A)**, it can easily be inferred up to 0.2 V sharp peaks of almost 1 are seen. From **Figure 3(A)** it is known that resonance voltage is 0.2 V and hence transmission is maximum till 0.2 V. Applying bias higher than peak voltage brings the device in NDR region i.e. off-resonant state. The appearance of off-resonant state results in less transmission of electrons which is seen in **Figure 4(A)** (0.3 and 0.5 V subplots) in the form of disappearance of sharp peaks. Further increase in bias will result in 0 transmission.

Figure 4(B) demonstrates the transmission coefficient plot at various barrier widths. Peaks in the 2 nm subplot are quite wider than peaks in the 15 nm subplot. Peak to peak distance is longer in the 2 nm subplot and it keeps on decreasing with each subplot. On increasing barrier width, resonant peaks become sharper and peak to peak distance becomes smaller. As barrier width increases, to get in or out of quantum well electrons require specific energy. Hence the lifetime of resonance increases. A longer

lifetime corresponds to sharper resonance [14]. The observations made are in accordance with the results stated by Zaharim *et al.* [17].

The transmission coefficient characteristics portrayed in **Figure 4(C)** shifted towards higher energy on increasing the temperature. More energy is required to get the same value of the transmission coefficient when the temperature is increased. Shen *et al.* [32] recognized that as an effect of scattering, peak transmission monotonically decreases with temperature. Normally, scattering pulls down electron waves and reduces transmission probability.

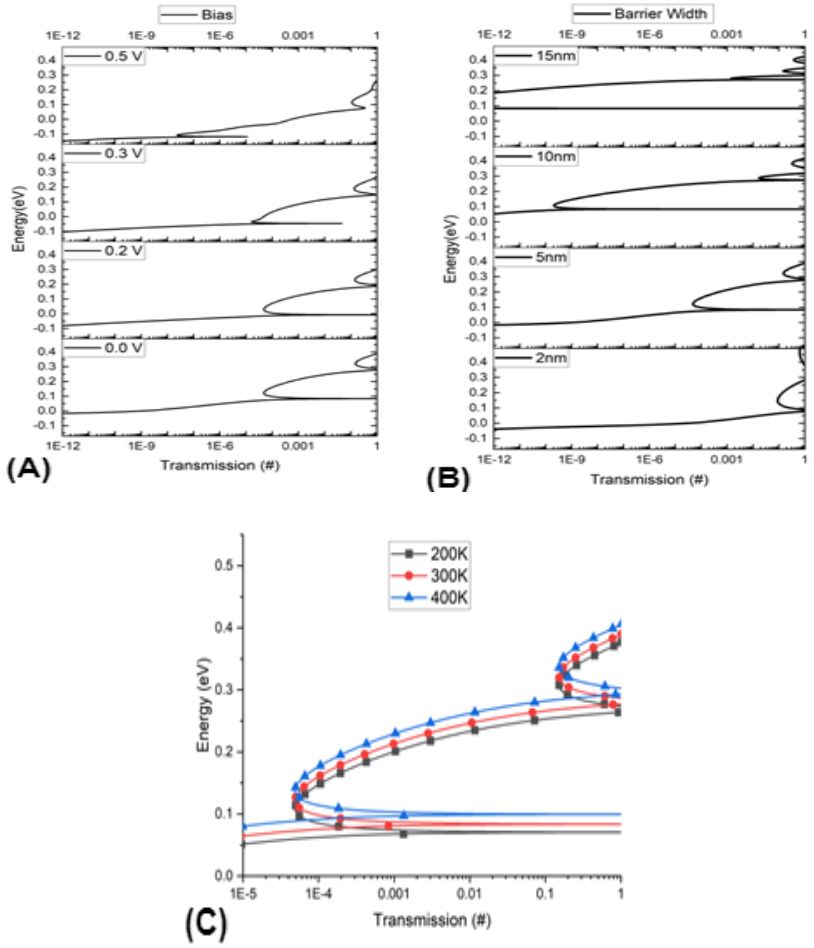

Figure 4 Energy vs transmission (A) varying bias, (B) varying barrier width and (C) varying temperature.

Resonance energy

The energies at which the barrier structure is totally transparent for the particle transmission and the particles can tunnel through the well are called resonance energies. The value of transmission coefficient is 1 for these resonance energies. **Figure 5** shows various plots of resonance energy vs bias on different parameters.

From **Figure 5(A)**, it can be observed that with the increase in temperature the resonance energy keeps on increasing. For example, it can be observed that the energy at 0.0 V, at 200 K the resonance energy is approximately 0.07 and 0.26 eV while at 300 K it is approximately 0.1 and 0.3 eV. Also, it is worth noting that with the increase in bias the resonance energy at a particular temperature decreases. This happens because, with the increase in applied bias voltage, conduction band offset is observed in **Figure 3(A)** which reduces the resonant energy level. Thus it can be said that with the increase in bias the height of the barrier reduces and so the energy of resonance can be observed from **Figure 5**. At temperature 300 K, for the first resonance energy level, the resonance energy is 0.1 eV at 0.0 V which is reduced to −0.1 eV at 0.5 V and similar work can also be observed from the work of Almansour and Dakhlaoui [18].

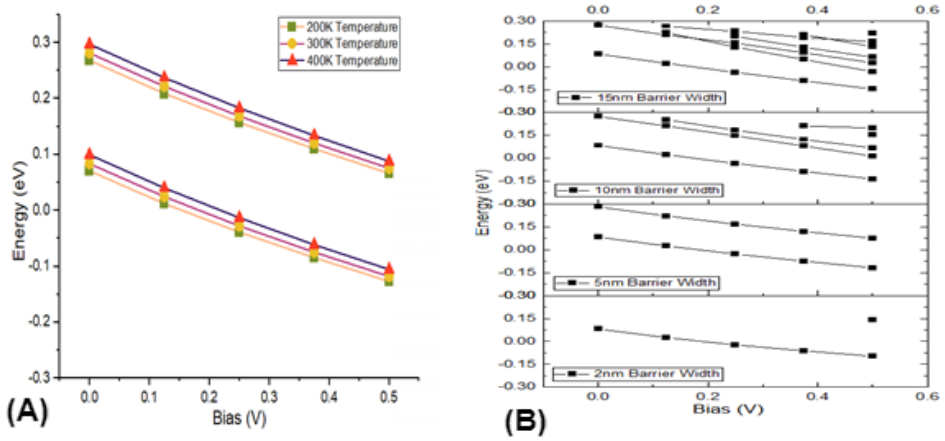

Figure 5 Energy vs bias (A) varying temperature and (B) varying barrier width.

For a resonant tunneling diode, with the increase in barrier width, the confinement of electrons in the well is made stronger due to which the lifetime of the resonance increases. Because of that sharper and more peaks are observed in **Figure 4(B)** with increasing barrier width as the maximum number of states become confined in well. Since each peak corresponds to a resonance energy level, with increasing barrier width more resonance energy levels can be seen in **Figure 5(B)**. For example, when the barrier width is 2 nm, there is only 1 resonance energy level while at a barrier width of 5 nm it can be observed 2 resonance energy levels. A similar study was done by Das and Parai [33] where they showed that bias reduces the heights of barriers, the right hand 1 particular, as well as the energy of the resonance. With the increase in resonance, more tunneling occurs in the diode therefore producing more forward current. Thus resonant tunneling diode is considered among the fastest devices because tunneling is very fast and not transit time-limited.

Triple barrier RTD and six barrier RTD

As shown in **Figure 1(B)**, the structure of triple barrier RTD consists of 2 quantum wells sandwiched among the barriers, which are connected with the spacer layers. The spacer's layers are connected with the GaAs contacts. This device consists of 3 barriers, 2 wells, spacer layers and contacts with individual material properties same to that of double barrier RTD. Similarly, six barrier RTD consists of six barrier and 5 quantum wells as can be seen in **Figure 1(C)**.

Conduction band

For triple barrier RTD, conduction band energy varies in the same way as double barrier RTD. In triple barrier RTD, there are 2 quantum wells as compared to double barrier RTD. On increasing the number of barriers, the number of quantum wells increases by one as observed in **Figure 6(A)**. The energy in the conduction band decreases similarly as observed in double barrier RTD on increasing bias or barrier width or well width. Similar results are observed in **Figure 6(B)** for six barrier RTD.

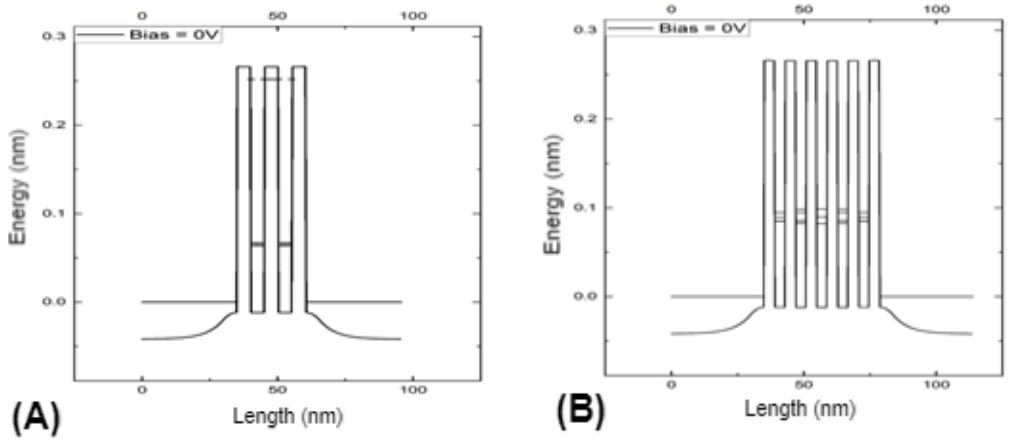

Figure 6 Conduction band (A) for triple barrier and (B) for six barrier.

Current density

The simulation on triple barrier RTD showed the occurrence of the NDR region at a very low voltage when compared with double barrier RTD. The current density increases linearly and reaches its peak at 0.015 V and then decreases rapidly similar to the simulated graph in double barrier RTD and achieves a minimum at 0.06 V. However, the peak current density is much lower in triple barrier RTD. Similar observations were also made by Almansour [19] where they found the peak to be at 0.01 V for triple barrier RTD. Also, the slope of current density obtained in **Figure 7(A)** is higher than the slope obtained in **Figure 3(A)**.

Similarly, when the simulations are performed for six barrier RTD, the peak current density in the six barrier obtained is the lowest as can be shown from **Figure 7(B)**. The peak current density is observed at 0.015 V and the valley current is observed at 0.03 V. The current density vs bias graph for six barrier RTD attains a similar shape as obtained in the double barrier and triple barrier RTD.

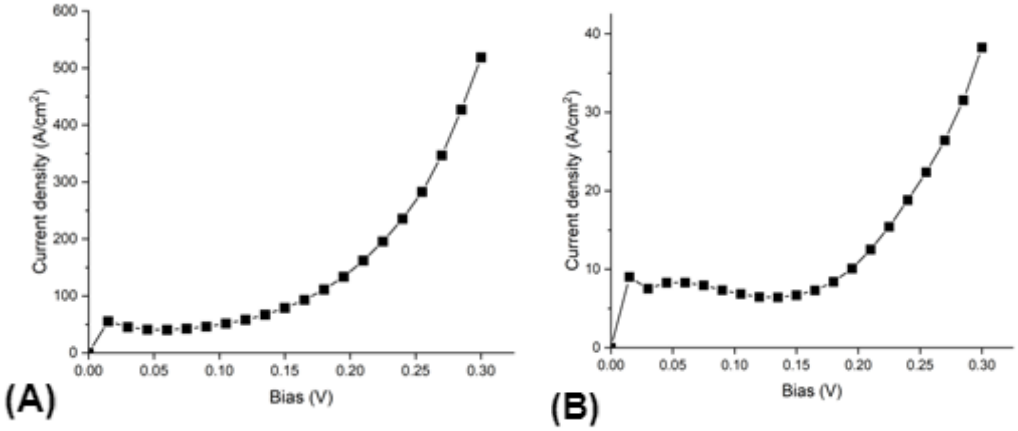

Figure 7 Current density vs bias (A) for triple barrier and (B) for six barrier.

Transmission coefficient

On increasing the number of barriers, the value of the transmission coefficient decreases in the energy range off-resonance condition. From **Figure 8(A)** it can be interpreted that transmission peak first decreases with the electric field and then increases to reach unity among resonance spectra. In triple barrier RTD, there is an addition of one more resonance energy state as compared to double barrier RTD (**Figure 6(A)** −0 V bias) i.e. number of peaks increased. The transmission spectrum has a Lorentzian-like shape which is similar to double barrier RTD [12]. With the increase in bias or temperature or barrier width, similar effects on the transmission coefficient as was seen in double barrier RTD was observed.

Similarly for six barrier RTD as it can be observed from **Figure 8(B)** that the number of peaks has increased.

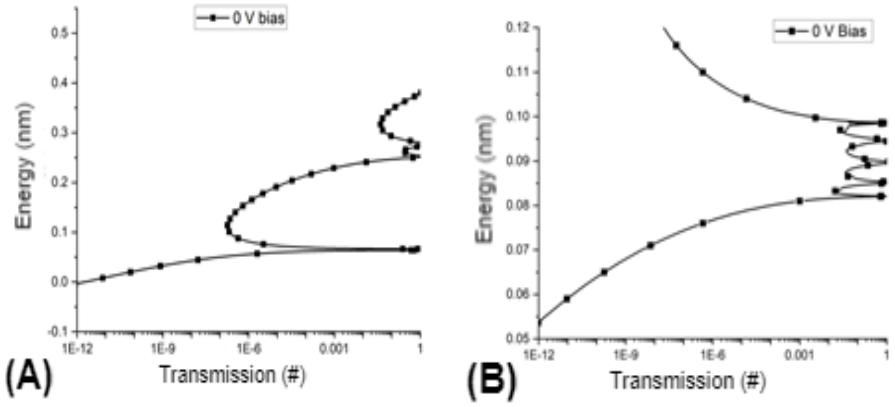

Figure 8 Energy vs trasmission coefficient (A) for triple barrier and (B) for six barrier.

Resonance energy

With the increase in the number of barriers, it can be seen from **Figures 9(A)** and **9(B)** that the number of resonance levels increases. This happens because the number of wells increases with the increase in the number of barriers and so more electrons tunnel through the well. So more peaks are observed in the transmission coefficient graph as observed in **Figures 8(A)** and **8(B)** under the same conditions and so more resonance energy levels as also discussed for the 2 barrier structure in **Figure 5(B)**. Similar results can also be seen for six barrier structures as shown in **Figure 9(B)**.

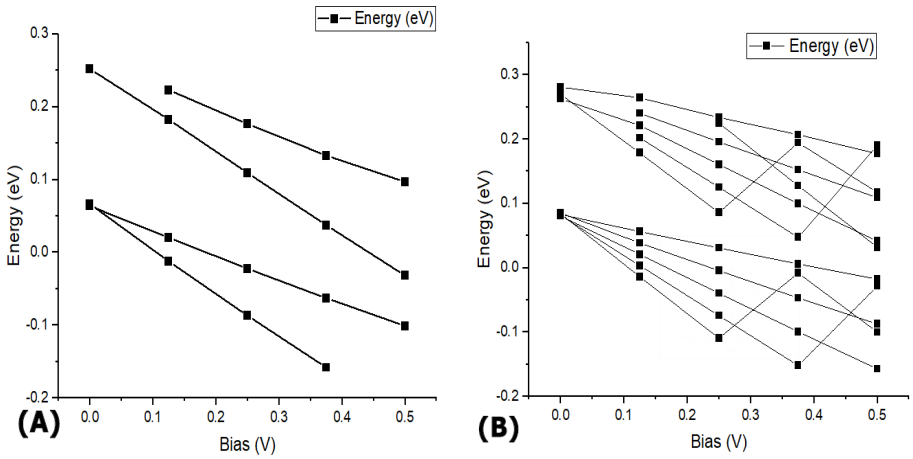

Figure 9 Resonance energy (A) for triple barrier and (B) for six barrier.

Conclusions

In this paper, the various properties of the GaAs-AlGaAs resonant tunneling diodes were investigated. The current density is observed to be higher in double barrier RTD when compared to triple barrier RTD. The peak current density in double barrier RTD is approximated to 3,165 A/cm^2 which is higher than the peak current density (55.5 A/cm^2) of triple barrier RTD and the peak current density (9 A/cm^2) for six barrier RTD. The appearance of the peak current density in triple barrier RTD is at 0.015 V but in double barrier RTD, it occurs around 0.2 V under standard conditions. The minimum current density observed in double barrier RTD is 1,286 A/cm^2 whereas in triple barrier RTD it is 40.5 A/cm^2 and in six barrier RTD it is 7.5 A/cm^2. The valley current density in the double barrier is observed at 0.3 V

whereas in triple barrier RTD it is observed at 0.06 V. The occurrence of the NDR region in the triple barrier RTD and in six barrier RTD is at low voltage when compared with double barrier RTD which opens significant areas for multistate logic and memory devices. With the increase in bias, a decrease in conduction band energy and a decrease in peak to peak distance in the transmission coefficient is observed. With the increase in doping concentration of contacts the charge carriers increases, leading to strictly increasing current density.

With the increase in the number of barriers there is a significant increase in the number of resonance levels, which leads to increased peaks in the transmission coefficient curve. The PVR ratio observes degradation from 2.46 in double barrier RTD to 1.37 in triple barrier RTD to 1.2 in six barrier RTD. On increasing temperature the peak to valley ratio observes degradation, the resonance energy increases. With increased barrier widths it is observed that the conduction band energy decreases, which leads to an increasing number of the resonance energy levels, sharper and increased no of peaks in the transmission coefficient curve. It is seen that the sharpness of resonance decreases with increasing electron energy and decreasing barrier width. RTD has opened up many doors for various applications.

References

[1] H Mizuta and T Tanoue. *The physics and applications of resonant tunnelling diodes*. Vol II. Cambridge University Press, Cambridge, 2006.

[2] S Saha, K Biswas and MR Hossain. Analysis of digital inverter using single and multiple GaAs/AlGaAs based double barrier resonant tunneling diode. *In*: Proceedings of the International Conference on Innovation in Engineering and Technology, Dhaka, Bangladesh. 2018, p. 1-6.

[3] J Lee, J Lee and K Yang. A low-power 40-Gb/s 1:2 demultiplexer IC based on a resonant tunneling diode. *IEEE Trans. Nanotechnol.* 2012; **11**, 431-4.

[4] SF Nafea and AAS Dessouki. An accurate large-signal SPICE model for resonant tunneling diode. *In*: Proceedings of the International Conference on Microelectronics, Cairo, Egypt. 2010, p. 507-10.

[5] AL Elgreatly, AA Shaaban and ESM El-Rabaie. Enhancement of drams performance using resonant tunneling diode buffer. *In*: Proceedings of the 1st International Conference on Information Technology, Computer and Electrical Engineering, Semarang, Indonesia. 2014, p. 16-20.

[6] M Asada and S Suzuki. Terahertz emitter using resonant-tunneling diode and applications. *Sensors* 2021, **21**, 1384.

[7] M Reddy. 1997, Schottky-collector resonant tunnel diodes for sub-millimeter-wave applications. Ph. D. Dissertation. University of California, Santa Barbara, California.

[8] TJ Slight and CN Ironside. Investigation into the integration of a resonant tunnelling diode and an optical communications laser: Model and experiment. *IEEE J. Quant. Electron*. 2007; **43**, 580-7.

[9] S Lin, D Wang, Y Tong, B Shen and X Wang. III-nitrides based resonant tunneling diodes. *J. Phys. D Appl. Phys.* 2020; **53**, 253002.

[10] LL Chang, EE Mendez and C Tejedor. *Resonant tunneling in semiconductors physics and applications.* Plenum Press, New York, 1991.

[11] TCLG Sollner, WD Goodhue, PE Tannenwald, CD Parker and DD Peck. Resonant tunneling through quantum wells at frequencies up to 2.5 THz. *Appl. Phys. Lett.* 1983; **42**, 588.

[12] H Yamamoto, Y Kanie, M Arakawa and K Taniguchi. Theoretical study of resonant tunneling in rectangular double-, triple-, quadruple-, and quintuple-barrier structure. *Appl. Phys. A* 1990; **50**, 577-81.

[13] VN Do, P Dollfus and V Lien Nguyen. Transport and noise in resonant tunneling diode using self-consistent Green's function calculation. *J. Appl. Phys.* 2006; **100**, 093705.

[14] G Klimeck. Tutorial 4a: High bias quantum transport in resonant tunneling diodes, Available at: https://nanohub.org/resources/11043, accessed January 2021.

[15] MM Singh, MJ Siddiqui, AB Khan and SG Anjum. Effect of barriers length and doping concentration on GaAs/AlGaAs RTD. *In*: Proceedings of the Annual IEEE India Conference, New Delhi, India. 2015.

[16] T Rong, LA Yang, Z Zhao, K Zhang and Y Hao. Theoretical modeling of triple-barrier resonant-tunneling diodes based on AlGaN/GaN heterostructures. *Phys. Status Solidi A* 2019; **216**, 1900471.

[17] WNN Zaharim, NZI Hashim, MFP Mohamed, AA Manaf and MAM Zawawi. Physical modelling of gallium nitride (GaN) based double barrier quantum well device. *In*: M Zawawi, S Teoh, N Abdullah, MM Sazali (Eds.). Lecture notes in electrical engineering. Vol 547. Springer, Singapor, 2019, p. 141-8.

[18] S Almansour and H Dakhlaoui. Electromodulation of the negative differential resistance in an AlGaAs/GaAs resonant tunneling diode. *J. Korean Phys. Soc*. 2019; **74**, 36-40.
[19] S Almansour. Theoretical study of electronic properties of resonant tunneling diodes based on double and triple AlGaAs barriers. *Results Phys.* 2020; **17**, 103089.
[20] EDG Castro, F Rothmayr, S Krüger, G Knebl, A Schade, J Koeth, L Worschech, V Lopez-Richard, GE Marques, F Hartmann, A Pfenning and S Höfling. Resonant tunneling of electrons in AlSb/GaInAsSb double barrier quantum wells. *AIP Adv*. 2020; **10**, 055024.
[21] S Sawai and K Narahara. Submillimeter-wave multiphase oscillation using traveling pulses in a resonant-tunneling diode-oscillator lattice. *J. Infrared Millimet. Terahertz Waves* 2021; **42**, 426-45.
[22] Y Nishida, N Nishigami, S Diebold, J Kim, M Fujita and T Nagatsuma. Terahertz coherent receiver using a single resonant tunnelling diode. *Sci. Rep.* 2019; **9**, 18125.
[23] LL Chang, L Esaki and R Tsu. Resonant tunneling in semiconductor double barriers. *Appl. Phys. Lett.* 1974; **24**, 593.
[24] S Datta. Nanoscale device modeling: The Green's function method. *Superlattice. Microst.* 2000; **28**, 253-78.
[25] S Datta. The non-equilibrium Green's function (NEGF) formalism: An elementary introduction. *In*: Proceedings of the Digest. International Electron Devices Meeting, San Francisco, California. 2002, p. 703-6.
[26] SL Yadav and H Najeeb-ud-din. A simple analytical model for the resonant tunneling diode based on the transmission peak and scattering effect. *J. Comput. Electron.* 2020; **19**, 1061-7.
[27] HH Park, Z Jiang, AG Akkala, S Steiger, M Povolotskyi, TC Kubis, JMD Sellier, Y Tan, SG Kim, M Luisier, S Agarwal, M McLennan, G Klimeck and J Geng. Resonant tunneling diode simulation with NEGF, Available at: https://nanohub.org/resources/rtdnegf, accessed January 2021.
[28] A Vercik, YG Gobato, M Mendoza and PA Schulz. Transport and optical properties of resonant tunneling structures. *Braz. J. Phys.* 2002; **32**, 331-3.
[29] KJP Jacobs, BJ Stevens, R Baba, O Wada, T Mukai and RA Hogg. Valley current characterization of high current density resonant tunnelling diodes for terahertz-wave applications. *AIP Adv*. 2017; **7**, 105316.
[30] D Banasree, P Manas and M Saikat. Effects on IV characteristics of RTD due to different parametric variations. *In*: Proceedings of the Devices for Integrated Circuit, Kalyani, India. 2017, p. 257-61.
[31] I Sanyal and MD Sarkar. Parameter optimization of a single well nanoscale resonant tunneling diode for memory applications. *In*: Proceedings of the IEEE International Conference on Electron Devices and Solid-State Circuits, Singapore. 2015, p.439-42.
[32] GD Shen, DX Xu, M Willander and GV Hansson. Analysis of resonant-tunneling transport. *Phys. Rev. B* 1992; **45**, 9424.
[33] B Das and MK Parai. Influence on characteristics of RTD due to variation of different parameters and material properties. *Int. J. High Speed Electron. Syst.* 2017; **26**, 1740022.